Regulation of ENaC trafficking in rat kidney

Gustavo Frindt,[1] Diego Gravotta,[2] and Lawrence G. Palmer[1]

[1]Department of Physiology and Biophysics and [2]Margaret Dyson Vision Research Institute, Department of Ophthalmology, Weill Cornell Medical College, New York, NY 10065

The epithelial Na channel (ENaC) forms a pathway for Na^+ reabsorption in the distal nephron, and regulation of these channels is essential for salt homeostasis. In the rat kidney, ENaC subunits reached the plasma membrane in both immature and fully processed forms, the latter defined by either endoglycosidase H–insensitive glycosylation or proteolytic cleavage. Animals adapted to a low-salt diet have increased ENaC surface expression that is specific for the mature forms of the subunit proteins and is similar (three- to fourfold) for α, β, and γENaC. Kidney membranes were fractionated using differential centrifugation, sucrose-gradient separation, and immunoabsorption. Endoplasmic reticulum membranes, isolated using an antibody against calnexin, expressed immature γENaC, and the content decreased with Na depletion. Golgi membranes, isolated with an antibody against the cis-Golgi protein GM130, expressed both immature and processed γENaC; Na depletion increased the content of processed γENaC in this fraction by 3.8-fold. An endosomal compartment isolated using an antibody against Rab11 contained both immature and processed γENaC; the content of processed subunit increased 2.4-fold with Na depletion. Finally, we assessed the content of γENaC in the late endocytic compartments indirectly using urinary exosomes. All of the γENaC in these exosomes was in the fully cleaved form, and its content increased by 4.5-fold with Na depletion. These results imply that stimulation of ENaC surface expression results at least in part from increased rates of formation of fully processed subunits in the Golgi and subsequent trafficking to the apical membrane.

INTRODUCTION

The epithelial Na channel (ENaC) is responsible for Na^+ reabsorption in the distal portions of the mammalian nephron (Garty and Palmer, 1997; Kellenberger and Schild, 2002). Up-regulation of these channels largely mediates the control of extracellular fluid volume by the mineralocorticoid aldosterone (Verrey et al., 2008). In rat cortical collecting ducts (CCDs), a low-Na diet dramatically increased the number of conducting channels in the apical membrane (Pácha et al., 1993). Although the hormone exerts some transcriptional control over channel expression, in the kidney, this is limited to the α subunit; the β and γ subunits are not induced (Asher et al., 1996; Escoubet et al., 1997; Stokes and Sigmund, 1998). Changes in protein levels follow the same pattern: the overall abundance of αENaC increased, with little change in the total amounts of β or γENaC (Masilamani et al., 1999; Ergonul et al., 2006). The augmentation of αENaC protein content is not sufficient to increase channel activity (Frindt and Palmer, 2012), indicating that increased synthesis of this subunit does not drive the elevation of channel function. Significant portions of the αENaC and γENaC subunits underwent shifts in apparent molecular mass consistent with proteolytic cleavage of the N terminus (Masilamani et al., 1999; Ergonul et al., 2006).

A shift in the location of channel protein from an intracellular compartment to the cell surface underlies an important part of the up-regulation process. This idea was first suggested by immunocytochemistry, which showed migration of ENaC protein from a diffuse perinuclear pattern to the apical pole of the cells of the distal nephron in response to aldosterone administration or dietary Na deprivation (Masilamani et al., 1999; Loffing et al., 2000, 2001). Whole-kidney biotinylation experiments supported this view, indicating a significant increase in expression at the cell surface under these same circumstances (Frindt et al., 2008; Frindt and Palmer, 2009).

As the increased surface expression is not the result of changes in the overall abundance of channel protein, it is likely caused by changes in the trafficking processes. The steps involved in hormone-dependent ENaC trafficking are unclear. In one scenario, aldosterone increases the surface lifetime of the channels by inhibiting ubiquitination and retrieval of ENaC from the cell surface (Staub et al., 1997, 2000; Snyder et al., 2002, 2005). Increased surface densities could also arise from stimulation of processing and forward trafficking to the apical membrane (Liang et al., 2010); the two ideas are not mutually exclusive. Previous studies have relied on cell lines and heterologous expression

Correspondence to Lawrence G. Palmer: lgpalm@med.cornell.edu

Abbreviations used in this paper: CCD, cortical collecting duct; DTT, dithiothreitol; ENaC, epithelial Na channel; EndoH, endoglycosidase H.

The Rockefeller University Press $30.00
J. Gen. Physiol. Vol. 147 No. 3 217–227
www.jgp.org/cgi/doi/10.1085/jgp.201511533

systems. Here, we address these issues using procedures to isolate various intracellular membrane compartments from rat kidneys and analyze them for ENaC content. The results are consistent with activation of forward processing of the channels as a major factor in the increased surface expression.

MATERIALS AND METHODS

Animals

All procedures using animals were approved by the Institutional Animal Care and Use Committee of Weill-Cornell Medical College. Female Sprague-Dawley rats (200–350 *g*; Charles River Laboratories) were raised free of viral infections. Animals were fed for 6–8 d with a Na-deficient rat diet (MP Biomedicals) or matched diets containing 1% NaCl (control Na) or 5% NaCl (high Na).

Rat kidney biotinylation

Renal plasma membranes were biotinylated in situ as described previously (Frindt et al., 2008; Frindt and Palmer, 2009) with some modifications. Kidneys were perfused with 0.5 mg/ml sulfosuccinimidyl-2-[biotinamido]ethyl-1,3-dithiopropionate (sulfo-NHS-biotin; Campbell Science) through the descending aorta. The reaction was stopped and excess biotin was removed by further perfusion with TBS. At the end of the perfusion, the left kidney was quickly removed, minced with a razor blade, and homogenized with a tight-fitting Dounce in 8 ml lysis buffer containing 250 mM sucrose, 10 mM triethanolamine HCl, 1.6 mM ethanolamine, 0.5 mM EDTA, pH 7.40, and 60 µl protease-inhibitor cocktail (Sigma-Aldrich). The homogenate was sieved with a nylon mesh (100 µm) to separate intact tissue and then centrifuged at 100,000 *g* for 2 h to sediment a total membrane pellet. This was resuspended in 2 ml lysis buffer, aliquoted, and frozen at −70°C for later analysis.

For isolation of biotinylated proteins, 3 mg pellet protein was solubilized in 1.5 ml solubilization buffer containing 100 mM NaCl, 50 mM Tris-HCl, pH 7.4, 5 mM EDTA, 3% Triton X-100, 0.5 mM 4-(2-aminoethyl)benzenesulfonyl fluoride, and 10 µg/ml leupeptin. 0.4 ml of a 50% suspension of NeutrAvidin UltraLink beads (Pierce) was added to the solubilized proteins, and the mixture was gently rocked overnight at 4°C. The next day, the beads were washed three times with solubilization buffer containing 1% Triton X-100, twice with high-salt solubilization buffer containing 500 mM NaCl and 0.1% Triton X-100, and twice with 10 mM Tris-HCl, pH 7.4. The packed beads were then suspended in 60 µl of 500 mM dithiothreitol (DTT) and incubated for 15 min at 75°C to release the biotinylated proteins by cleaving the disulfide bonds of the reagent. After sedimentation of the beads with a brief centrifugation, 60 µl supernatant was collected and prepared for electrophoresis by adding 20 µl of 4× sample buffer and heating for 10 min at 70°C. For electrophoresis, each lane of the gel was loaded with 40 µl (β or γENaC) or 60 µl (αENaC) of this mixture.

Deglycosylation

To assess glycosylation patterns, surface proteins were treated with the enzymes endoglycosidase H (EndoH) or PNGaseF (New England Biolabs) according to the manufacturer's instructions. In brief, proteins bound to NeutrAvidin beads (see previous section) were eluted in 120 µl of 375 mM DTT and 10 mM Tris-HCl, pH 7.4, at 65°C for 30 min. 60 µl of the eluate was mixed with 6 µl of 10× glycoprotein denaturing buffer and divided into three aliquots of equal volume. One of these was mixed with 3 µl of 10× G7 buffer, 4 µl of 10% NP-40, and 3 µl PNGaseF solution. The second was mixed with 3 µl of 10× G5 buffer, 4 µl H_2O, and 3 µl EndoH solution. The third was mixed with 3 µl of 10× G7 buffer, 4 µl of 10% NP-40, and 3 µl of 50% glycerol. The three aliquots were incubated at 37°C for 1 h before preparation for SDS-PAGE.

Western blots

Polyclonal antibodies against the α, β, and γ subunits of the rat ENaC were described previously (Ergonul et al., 2006; Frindt et al., 2008; Frindt and Palmer, 2009). Protein in the membrane fractions and homogenates was measured (BCA kit; Pierce Biotechnology). Samples containing 0.5 mg of protein in 65 µl of lysis buffer were prepared for electrophoresis with 25 µl 4× sample buffer and 10 µl 10× sample reducing agent (Invitrogen) and denatured at 70°C for 10 min. For SDS-PAGE, 4–12% bis-Tris gels (Invitrogen) were loaded with 30–40 µg of protein/lane (β or γENαX) or 50–60 µg of protein/lane (αENaC).

For immunoblotting, the proteins were transferred electrophoretically from unstained gels to polyvinylidene fluoride membranes. After blocking with casein (Invitrogen), membranes were incubated overnight at 4°C with primary antibodies at 1:500 (αENaC) or 1:1,000 (β or γENαX) dilutions. Bound antibodies were detected using anti–rabbit IgG conjugated with alkaline phosphatase and detected with a chemiluminescence substrate (Western Breeze; Invitrogen) on autoradiography film (Denville Scientific). Films were scanned with Epson Scan software, and band densities were quantitated using Photoshop (Adobe Systems). Densities were within the linear range of the detection system (Ergonul et al., 2006).

Differential and density-gradient centrifugation

To partially purify membrane fractions, rat kidney microsomes were first separated using differential and density-gradient centrifugation. All steps were performed on ice or in a cold room. Each solution used contained protease-inhibitor cocktails. Kidneys from two rats were harvested and homogenized in lysis buffer with a Dounce using six strokes with a loose pestle and six more with a tight pestle. The homogenates of four kidneys were pooled into a single 50-ml sample and centrifuged at 1,000 *g* for 10 min to obtain a 1K pellet. The supernatant was centrifuged at 4,000 *g* for 20 min. The 4K supernatant was centrifuged at 17,000 *g* for 20 min. The resulting 17K supernatant was spun at 100,000 *g* for 60 min to produce a 100K pellet. Contents of markers for various subcellular compartments in the homogenate and different pellets are shown in Fig. S2.

In subsequent experiments comparing kidney membranes from rats fed control and low-Na diets only 1K, 4K, and 100K pellets were produced. The 1K and 100K pellets were resuspended in lysis buffer and their sucrose concentrations adjusted to 1.4 M using a 2.4 M solution. The final volumes were 28 ml for 1K and 14 ml for the 100K pellets. 14 ml of each suspension was placed at the bottom of 38-ml centrifuge tubes and overlaid by discontinuous sucrose gradients containing 1.2, 1.1, 1.0, 0.9, 0.8, 0.4, and 0.25 M sucrose solutions. These solutions contained 0.5 mM EDTA and 10 mM triethanolamine HCl, pH 7.4. Their volumes started at 5 ml for 1.2 M sucrose and decreased progressively to 3 ml. The gradients were then centrifuged at 98,000 *g* for 3 h.

At the end of the centrifugation, the material at each interface was collected with a pipette connected to a syringe, diluted with 1–1.5 volumes of cold buffer containing 60 mM NaCl, 0.5 mM EDTA, and 10 mM triethanolamine HCl, pH 7.4, and centrifuged at 70,000 rpm for 10 min. The pellets were resuspended in 25–400 µl of lysis buffer, depending on their size, and frozen at −70°C for later analysis. The samples were labeled A to F starting with the lightest sample at the 0.4/0.8M sucrose interface and ending with the 1.2/1.4M interface; sample G contained material that remained in the 1.4M layer. The contents of markers for different subcellular compartments is shown in Figs. S3 and S4. Some of

these fractions were further used to immunoisolate membranes containing calnexin, GM-130, or Rab11.

Immunoabsorption

Isolation of membranes containing Rab11 or calnexin followed previous protocols (Trischler et al., 1999; Butterworth et al., 2012). For isolation of ER membranes, we used a rabbit anti-calnexin antibody (Enzo Life Sciences) raised against a peptide from the C terminus of dog calnexin. The anti-calnexin IgG was bound to protein G magnetic beads (Dynabeads; Novex Life Technologies). 1.5 mg washed beads was suspended in 1 ml buffer I (PBS containing 0.5% IgG-free albumin, 1 mM EDTA, and 0.4M sucrose, pH 7.4) with 10 µg IgG for 3 h with gentle rocking at 4°C. Control beads were coated with 10 µg anti-AII receptor 1A antibody (Santa Cruz Biotechnology, Inc.). Next, the beads were washed four times with 1.5 ml buffer I, resuspended in 0.6 ml of the same buffer mixed with 1 mg of protein from fraction F (1.2 M/1.4 M sucrose interface) of the 1K pellet and incubated overnight with gentle rocking at 4°C.

The following day, the beads were washed three times with 1.5 ml buffer I and twice with 1 ml buffer II (the same as buffer I, without albumin) and transferred to a clean tube. The fluid over the beads was drained and the captured proteins eluted by resuspending the beads in 45 µl of 50 mM Tris-HCl, pH 7.8, containing 1.5% (vol/vol) Triton X-100 and rocking at 4°C for 40 min. The supernatant was mixed with 8 µl 10× sample reducing agent and 20 µl 4× sample buffer enriched with an additional 8% SDS and heated at 70°C for 10 min. For SDS-PAGE, 60 µl was loaded per lane. The beads were then treated with 60 µl sample buffer with reducing agent and heated at 70°C for 15 min to elute the calnexin and its antibody. 60 µl of this eluate was also analyzed by SDS-PAGE.

The pull-down of Rab11-containing endosomes followed a variation of the aforementioned procedure. 0.25 mg of membrane fraction E (1.1/1.2M sucrose interface) of the 100K pellet was suspended in 0.5 ml buffer I with 2.5 µg anti-Rab11 antibody (Invitrogen) or the irrelevant control antibody. The mixture was incubated for 2 h with gentle rocking at 4°C. Subsequently, protein G–coated magnetic beads (3 mg) were added to the mixture and incubated overnight. After washing the beads, the captured proteins were eluted for 15 min at 70°C with 50 µl sample buffer with DTT. The eluate was used directly for SDS-PAGE.

The recovery of γENaC and marker proteins from immune absorption of sucrose-gradient fractions is shown in Figs. S5 and S7. 9% of calnexin was recovered from fraction F of the 1K pellet with the calnexin-coated beads (Fig. S5) using SDS. In Triton-X 100 eluates from the same beads, we recovered 2% of the total uncleaved γENaC in the starting material. This implies that ∼20% of this form of the subunit was contained in a calnexin-expressing compartment. A similar analysis of the Rab11 pull-down assay (Fig. S7) indicated a recovery of 44% of Rab11 from fraction E of the 100K pellet, 7% of full-length γENaC, and 8% of cleaved γENaC. This suggests that 15–20% of γENaC is in the Rab11-containing compartment.

The specificity of the immune-isolation procedures is illustrated in Figs. S6 and S8. The pull-down using anti-Rab11 contained very small amounts of plasma membrane (using syntaxin 4) or ER (using ribophorin; Fig. S6). The pull-down using anti-calnexin contained the ER marker ribophorin, as expected, but not syntaxin 4 or Rab11 (Fig. S8). The paucity of isolated material prevented us from a systematic inventory or a more quantitative assessment.

The protocol for pull-down of GM130-containing cis-Golgi membranes was a variation on the aforementioned schemes. First, a fraction enriched in Golgi membranes was prepared according to the method of Matsuda et al. (1983). Kidneys from two rats were homogenized in lysis buffer (see Rat kidney biotinylation). Homogenates were centrifuged at 400 *g* for 10 min. The resulting supernatants were spun at 3,000 *g* for 10 min. The new supernatants were adjusted to 50% sucrose using 2.4 M sucrose solution. 18 ml of this mixture was placed in the bottom of a 38-ml centrifuge tube and overlaid with a discontinuous gradient consisting of 6 ml each of 45%, 40%, and 30% sucrose and 5 ml lysis buffer. The gradients were centrifuged at 96,000 *g* for 131 min. Material at each interface, plus the 50% sucrose layer, was collected, diluted with an equal volume of cold deionized H_2O, and centrifuged at 105,000 *g* for 30 min. The resulting pellets were suspended in 40–400 µl of lysis buffer depending on their size.

The material at the 30%/40% sucrose interface was used to isolate membranes of the cis-Golgi by immunoabsorption with a rabbit monoclonal anti-GM130 antibody (Abcam). 0.5 mg of membrane protein was suspended in 1 ml buffer I with protease inhibitors and incubated for 2 h at 4°C with gentle rocking with 2 µg of anti-GM130 IgG or as a negative control with 2 µg anti-AII receptor 1A. Next, 2 mg of protein G–coated magnetic beads was added and the mixture was incubated overnight. The next day, the beads were washed as described for the calnexin pull-down, and the captured proteins were eluted with 100 µl sample buffer at 75°C for 20 min. The eluates were analyzed by SDS-PAGE loading 50 µl/lane. The paucity of material obtained with this protocol prevented an analysis of its recovery or specificity.

Urinary exosomes

Preparation of urinary exosomes followed the procedure of McKee et al. (2000). Rats were housed in metabolic cages and urine was collected on ice for 4–5 h. The collection tubes contained 20 µl protease inhibitor cocktail. Samples were centrifuged for 5 min at 1,000 *g* to sediment debris and intact cells. Creatinine in the supernatant was measured using a colorimetric kit (BioAssay Systems) following the manufacturer's instructions. The supernatant was centrifuged at 200,000 *g* for 2 h. The resulting pellet was suspended in 100–200 µl sample buffer. The volume was proportional to the creatinine content in the collected urine. The sample was then processed as described in the section on Western blots. 10 µl of sample, representing exosomes from a volume of urine containing 70 µg creatinine, was loaded in each lane.

Online supplemental material

Fig. S1 shows a Western blot of αENaC from whole-kidney microsomes. Fig. S2 shows representative results of differential centrifugation of kidney homogenates. Fig. S3 shows sucrose density separation of low-speed pellets from differential centrifugation. Fig. S4 shows sucrose density-gradient separation of high-speed pellets from differential centrifugation. Figs. S5 and S6 show the recovery from and specificity of the anti-calnexin immune-isolation procedure. Figs. S7 and S8 show the recovery from and specificity of the anti-Rab11 immunoisolation procedure. Fig. S9 illustrates the effects of PNGaseF and EndoH on urinary exosomes. Online supplemental material is available at http://www.jgp.org/cgi/content/full/jgp.201511533/DC1.

RESULTS

Rats were fed a control, high-Na, or low-Na diet for 7 d. To assess the biochemical state of ENaC subunits in the plasma membrane, we isolated renal surface proteins by perfusing the kidneys with an impermeant biotin reagent and capturing labeled proteins using NeutrAvidin beads. We treated the surface fractions with either PNGaseF, an amidase that digests all N-glycan chains from glycoproteins, or with EndoH, which specifically attacks the high-mannose core of incompletely glycosylated proteins

(Maley et al., 1989). The results for βENaC are shown in Fig. 1 A. With either a control or high-Na diet, PNGaseF and EndoH had similar effects on the subunit, reducing the apparent molecular mass from ∼90 to ∼70 kD. Thus, under these conditions, most of the subunits that reach the surface have an immature glycosylation pattern. When the animals were Na depleted, the apparent molecular mass of the subunit increased, consistent with more complete glycosylation. In addition, a large fraction of βENaC at the surface was incompletely deglycosylated by EndoH, indicating the presence of the maturely glycosylated protein.

Results with γENaC were similar, although more complex, because of two forms of this subunit (full-length and cleaved). In whole-kidney extracts under control conditions, most γENaC is in the full-length, 80-kD form (Masilamani et al., 1999; Ergonul et al., 2006). However, as reported previously (Frindt et al., 2008), at the surface, the cleaved, 65-kD species predominates and increases in abundance with dietary Na depletion. The full-length form represents a small fraction of the total at the surface and decreases with Na depletion. This is unlikely to represent contamination by ENaC from intracellular organelles, as no biotinylation of markers of these membranes could be detected (Frindt et al., 2008). As shown in Fig. 1 B, both PNGaseF and EndoH decreased the apparent molecular mass of the full-length form by the same amount, from 80 to 68 kD. The cleaved form, in contrast, was resistant to EndoH treatment, decreasing in size from 65 to 50 kD with PNGaseF but to a lesser extend with EndoH. These data suggest that this form has mature glycosylation, consistent with the idea that proteolytic cleavage and final glycosylation both occur in the Golgi apparatus. Similar results were reported previously for ENaC in heterologous expression systems (Hughey et al., 2003).

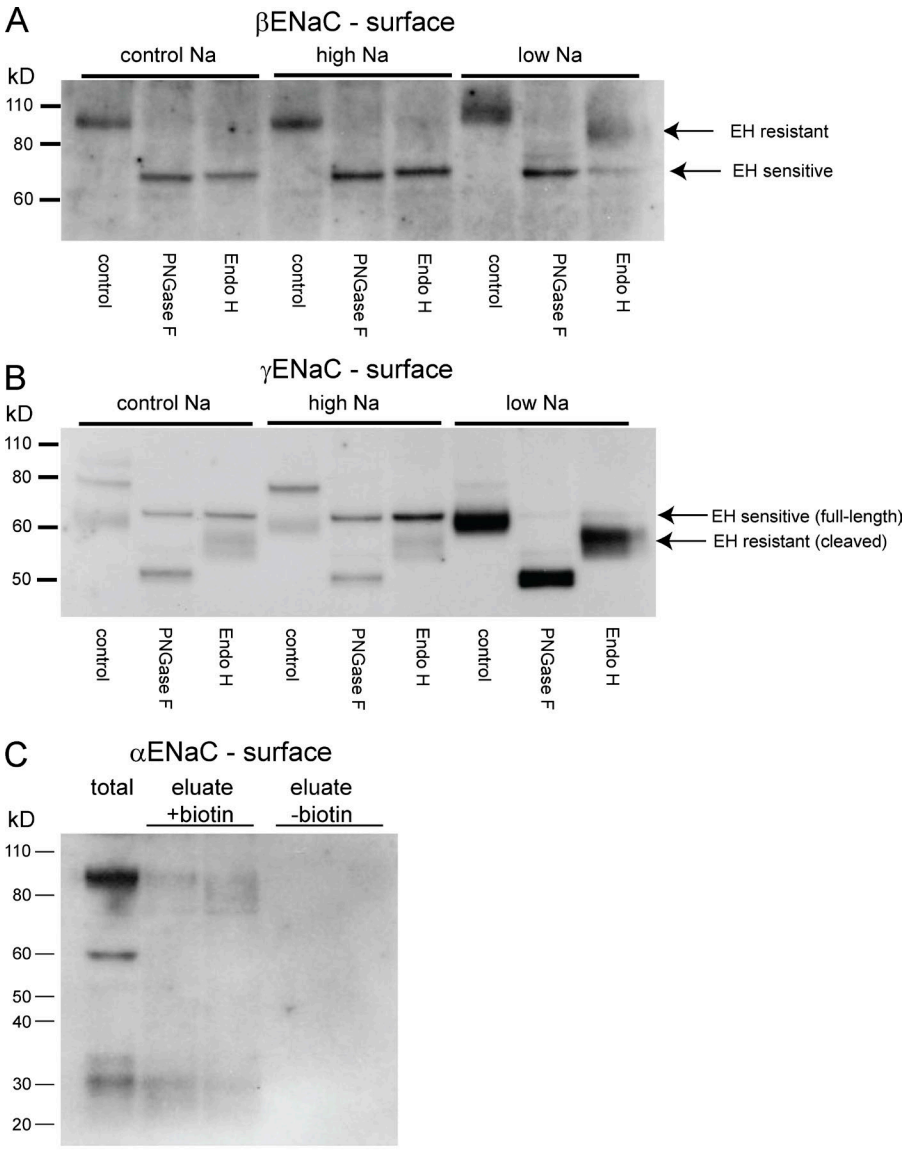

Figure 1. Expression of EndoH-sensitive and -resistant forms of ENaC at the cell surface. (A and B) Surface membrane fractions were isolated from biotinylated kidneys. These fractions were treated with either EndoH (to cleave high-mannose N-linked glycosylation trees) or PNGaseF (to cleave all trees). These products were separated using SDS-PAGE and probed with antibodies against the C terminus of βENaC (A) or γENaC (B). In both cases, EndoH (EH)-sensitive and -resistant forms were observed. EndoH-resistant subunits were much more abundant when animals were fed a low-Na diet. (C) Biotinylated fractions were probed with antibodies against the N termini of αENaC. Both full-length (∼90 kD) and cleaved (∼30 kD) forms of the subunit were detected, in addition to protein with a diffuse molecular mass of 75–90 kD. Eluates from nonbiotinylated kidney extracts did not have detectable signals.

We were previously unable to directly assess αENaC at the cell surface using the biotinylation approach because of nonspecific binding to NeutrAvidin beads. We overcame this problem by eluting material from the beads using DTT to break the S–S bond of the biotin reagent. As shown in Fig. 1 C, this process eluted both high molecular mass (75–95 kD) and low molecular mass (30 kD) forms of the subunit from the beads. A negative control eluate using membranes not exposed to biotin contained no detectable αENaC protein. The high-molecular-mass material was variable in both apparent size and in amount, generally running as a broad band at and below the putative full-length form of the subunit. The low-molecular mass material is similar in size to the N-terminal fragment of the α subunit observed in whole-kidney with Na depletion (Ergonul et al., 2006). We did not perform analysis of this material with glycosidases, as we could not clearly identify Endo-H sensitive and resistant forms in whole-cell extracts (Ergonul et al., 2006). However previous results with whole-kidney extracts indicated that full-length αENaC is EndoH-sensitive (Ergonul et al., 2006). We assume that, as with the γ subunit, cleaved αENaC represents the mature, fully processed form.

We next compared the surface expression of the presumed mature forms of the three subunits with control and low-Na diets. Based on the results in Fig. 1, we assayed for the cleaved (30 kD) form of αENaC (Fig. 2 A), the EndoH-resistant form of βENaC (Fig. 2 B), and the cleaved (65 kD) form of γENaC (Fig. 2 C). As shown in Fig. 2 D, all three of these forms increased by similar degrees (3.5-fold) with Na depletion. The analysis of αENaC is the least certain of the three because of a low signal-to-background ratio especially under control conditions. This was also the case when the total microsomal pellet was assayed (Fig. S1). However, the fold increase in the 30 kD subunit in the surface fraction (3.3-fold) is comparable to that in the microsomes (3.9-fold; Fig. S1), in the exosomes (4.3-fold; see Fig. 6) and in previous measurements in a fraction enriched in plasma membranes (4.3-fold; Frindt et al., 2008). Thus, although the overall pattern of expression at the surface is complex and different for each subunit, the fully processed subunits (which presumably represent active channels) appear to increase at the cell surface in stoichiometric amounts.

To better understand the trafficking events affected by Na depletion, we assayed various intracellular compartments for ENaC abundance. In any given compartment, the steady-state abundance will reflect the balance between rates of delivery of protein into and rates of removal from that compartment. This information may give insight into the nature of trafficking steps that result in increased surface expression of the channels.

In the case of the endoplasmic reticulum, the abundance will depend on rates of protein synthesis and export to the Golgi or to other organelles. We used an immunoabsorption approach to isolate vesicles derived from the endoplasmic reticulum. Fig. 3 (A and B) shows the control measurements using anti-calnexin antibody to interact with the ER membranes. This resulted in the pull-down of both calnexin itself (Fig. 3 A) as well as γENaC (Fig. 3 B). A control IgG resulted in no significant recovery of these proteins from the eluate. The paucity of material from the immunoisolation procedures limited the number of proteins that we could assay in these fractions. Therefore we focused the analysis on γENaC. This subunit was chosen for the ease of distinguishing mature and immature forms. All of the γENaC detected was in the uncleaved, incompletely processed form, as expected for a protein that has not

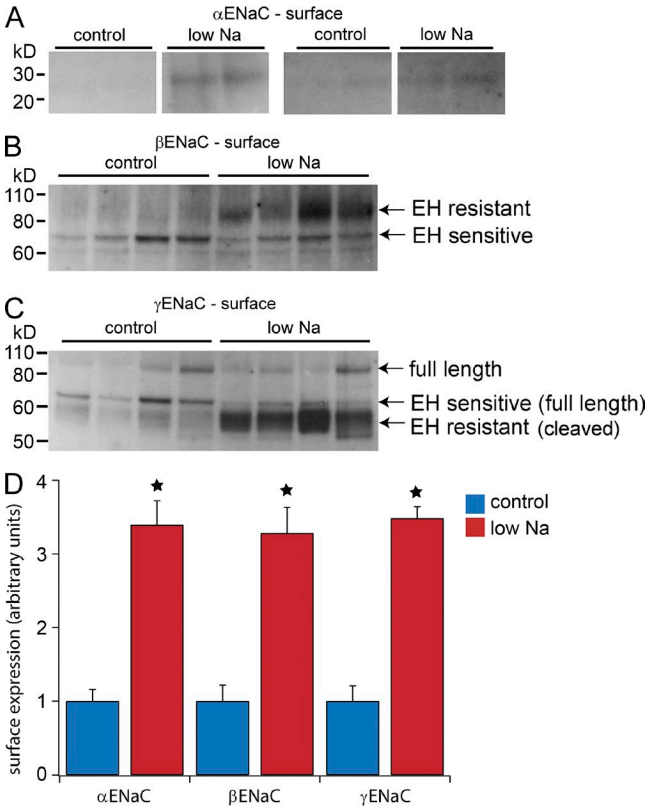

Figure 2. Effects of a low-Na diet on processed ENaC subunits at the cell surface. (A) For αENaC, the fully processed form was identified as the 30-kD cleaved species, which increased with Na depletion. Two gels from different experiments are shown. Noncontiguous portions of the same gel are compared, with intermediate portions excised for clarity. No further image processing was performed. (B) For βENaC, the EndoH (EH)-resistant form was strongly increased, whereas the EndoH-sensitive form was not significantly affected by Na depletion. (C) For γENaC, the EndoH-resistant form was strongly increased, whereas the EndoH-sensitive form was reduced by Na depletion. (D) Quantitation of the results in A–C. The cleaved form of αENaC and EndoH-resistant forms of βENaC and γENaC increased to similar extents with Na depletion (~3.5-fold over control levels). Results represent mean ± SEM of four independent experiments. *, $P < 0.05$ by *t* test.

entered the Golgi apparatus. The content of γENaC was decreased in the low-Na membranes compared with those of controls (Fig. 3 C). This is consistent with a scenario in which low Na stimulates the export of assembled channels out of the ER.

To test whether ENaC content changed downstream of the ER, we isolated Golgi membranes using antibodies against GM130, a resident membrane protein in the cis-Golgi. These vesicles contained both full-length and cleaved forms of γENaC (Fig. 4); the predominant form is full length. Because very little immature protein reaches the plasma membrane, these full-length subunits must be either undergoing processing or destined for degradation before reaching the apical surface. The cleaved subunit in the Golgi preparation appeared to be predominantly in a partially cleaved state, whereas the plasma membrane expresses the fully cleaved subunit. This agrees with the idea that γENaC is cleaved first by Golgi proteases such as furin and again later by extracellular or membrane-bound enzymes (Hughey et al., 2004a). A key finding in this figure is that Na depletion increases the amount of cleaved γENaC in the Golgi by a similar factor (three- to fourfold) as in the plasma membrane. This again suggests stimulation of forward trafficking of the subunit.

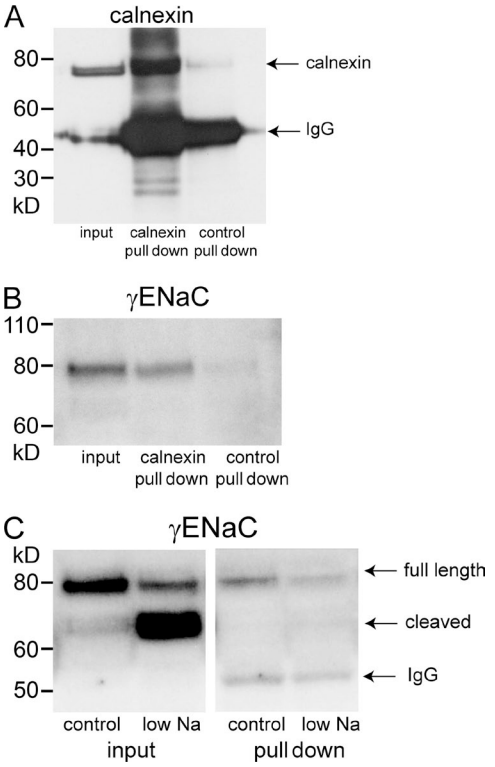

Figure 3. Pull-down of membrane proteins using anti-calnexin antibodies. Calnexin-containing microsomes from rat kidneys were partially purified using differential and density-gradient centrifugation (see Materials and methods). These fractions were incubated with protein G–coated beads primed with anti-calnexin antibody. (A) Significant amounts of calnexin were pulled down from the starting material (input) when beads were coated with anti-calnexin but not with control antibody. The bands at 55 kD represent the IgG species used for pull-downs. (B) Significant amounts of γENaC were pulled down from the starting material with anti-calnexin, but not with control antibody. Only the full-length species was detected. (C) Pull-down of membranes from kidneys of control and Na-depleted rats. The starting material contains both full-length and cleaved γENaC, with the full-length predominating under control conditions and the cleaved predominating after Na depletion. The membranes isolated with anti-calnexin contain only full-length subunits. The abundance decreased with Na depletion. The 55-kD bands represent the anti-calnexin IgG used for the pull-down. The results are representative of four independent experiments. Quantification is shown in Fig. 7.

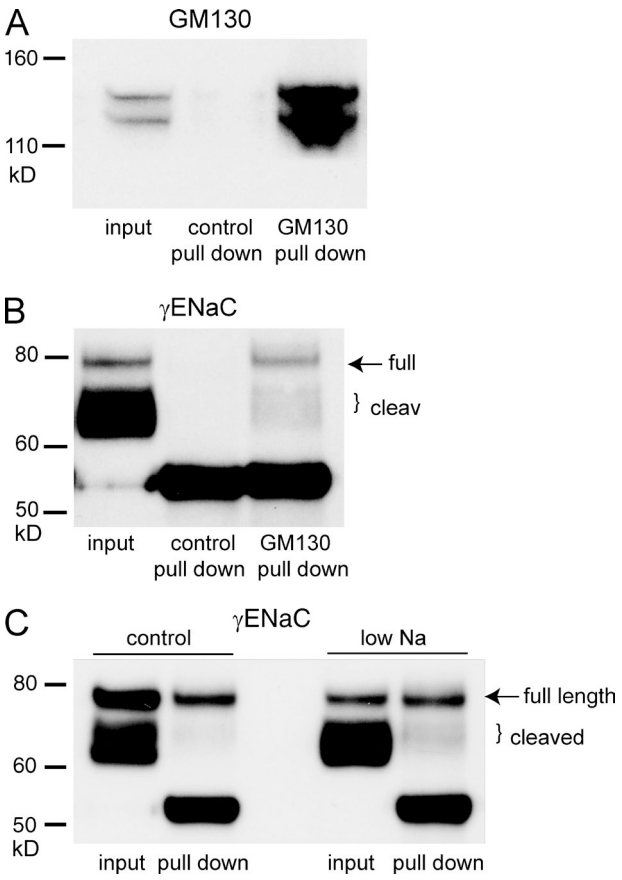

Figure 4. Pull-down of membrane proteins using anti-GM130 antibodies. Golgi-containing microsomes from rat kidneys were partially purified using differential and density-gradient centrifugation (see Materials and methods). These fractions were incubated with anti-GM130 antibody, and the antibody–membrane complexes were captured with protein G–coated magnetic beads. (A) Significant amounts of GM130 were pulled down from the starting material with anti-GM130 but not with control antibody. (B) Significant amounts of γENaC were pulled down from the starting material with anti-GM130 but not with control antibody. Both full-length and cleaved forms were detected. (C) Na depletion increased the amount of cleaved γENaC in GM130-containing vesicles. The 55-kD bands represent the anti-GM130 IgG used for the pull-down. The results are representative of four independent experiments. Quantification is shown in Fig. 7.

An increase in the number of channels at the surface could also be a consequence of decreased rates of retrieval from the plasma membrane, as suggested by effects of gain-of-function mutations involving Nedd4-2 ubiquitinase binding sites (Staub et al., 2000; Snyder, 2005). Changes in the rate of internalization from the surface could alter the content of endosomes. To test this, we isolated vesicles using antibodies against Rab11, a component of a subset of apical recycling endosomes in epithelia (Casanova et al., 1999; Wang et al., 2000). Butterworth et al. (2012) showed that in cultured mouse CCD cells, this compartment contains ENaC and helps to control apical surface expression. Fig. 5 (A and B) illustrate control experiments. Incubating light kidney membrane fractions complexed with antibody against Rab11 together with protein G–coated beads enabled the isolation of Rab11-containing (Fig. 5 A) and γENaC-containing (Fig. 5 B) vesicles, whereas using an irrelevant IgG as a negative control did not bring down either of these proteins. Fig. 5 C compares the pull-down of γENaC from kidneys of control and Na-depleted rats. There was considerably more of the mature form of the subunit in the endosomes of the animals on a low-Na diet. Thus, both the state of γENaC and its relative content were similar in the plasma membrane and the recycling endosomes. This could reflect rapid transfer from one compartment to the other.

Direct immunoisolation of late endosomes using anti-Rab7 antibodies was unsuccessful. We were however able to detect ENaC in urinary exosomes (Fig. 6). These vesicles are thought to derive from multivesicular bodies, structures late in the endocytic process (Pisitkun et al., 2004). All of the γENaC, as well as αENaC, was in a fully cleaved state in this fraction. To test whether the cleaved forms represent fully processed subunits, we examined the sensitivity of the γENaC in this fraction to EndoH. Fig. S9 shows that all of the γENaC in the exosomes is EndoH resistant, implying that it has passed through the Golgi apparatus. βENaC also appeared to be in a higher molecular mass, presumably fully glycosylated, form. The exosomes may therefore reflect a pathway for the selective export of the fully processed form of the channel protein from the cell. The amount of fully processed ENaC in the exosomes increased during Na restriction, again consistent with an overall increase in its formation. Here we assume constant rates of exosome excretion in the ENaC-containing cells.

Fig. 7 summarizes quantitative results from experiments illustrated in Figs. 2, 3, 4, 5, and 6. The amount of uncleaved γENaC in the ER decreases significantly with Na depletion. One interpretation of this observation is that movement from ER to Golgi accelerates under these conditions. At the same time, Na depletion increases the abundance of cleaved γENaC in all compartments from the Golgi to the urinary exosomes to similar extents. This suggests that acceleration of trafficking through the entire pathway underlies, at least in part, the increase in surface expression of the protein under these conditions.

DISCUSSION

The main conclusions of the work are (a) ENaC subunits with either mature (EndoH resistant) or immature (EndoH sensitive) glycosylation patterns reach the plasma membrane of rat kidneys; Na depletion

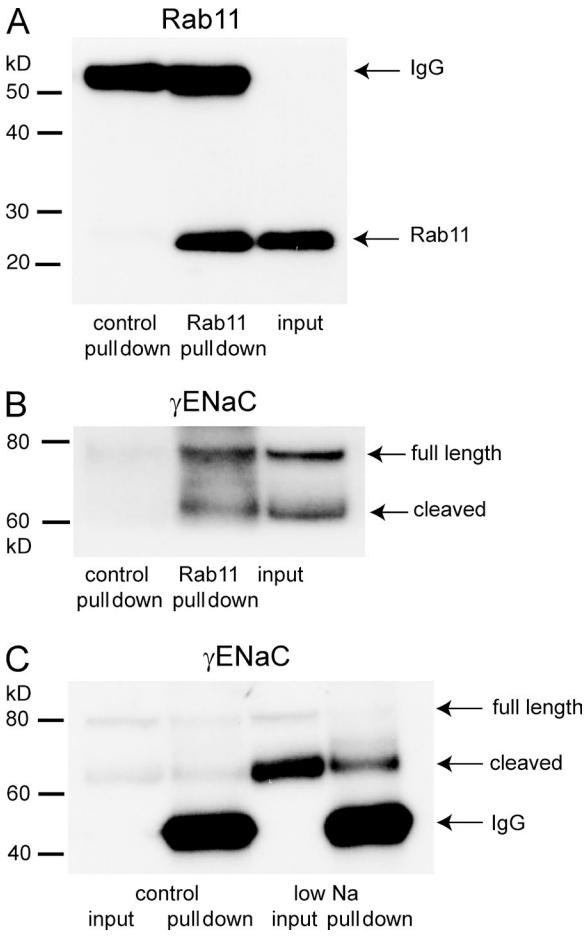

Figure 5. Pull-down of membrane proteins using anti-Rab11 antibodies. Rab11-containing microsomes from rat kidneys were partially purified using differential and density-gradient centrifugation (see Materials and methods). These fractions were incubated with anti-Rab11 antibody, and the antibody–membrane complexes were captured with protein G–coated beads. (A) Significant amounts of Rab11 were pulled down from the starting material ("input") when labeled with anti-Rab11 but not with a control antibody. The bands at 55 kD represent the IgG species used for labeling. (B) Significant amounts of γENaC were pulled down from the starting material when labeled with anti-Rab11 but not with control antibody. Both full-length (80 kD) and cleaved (60–65 kD) species were detected. (C) Na depletion increased the amount of cleaved γENaC in Rab11-containing vesicles. The 55-kD bands represent the anti-Rab11 IgG used for the pull-down. The results are representative of four independent experiments. Quantification is shown in Fig. 7.

specifically increases the former. (b) The abundance of the three mature subunits (EndoH resistant, proteolytically cleaved) increases in parallel. This presumably represents the pool of active, conducting channels in the apical membrane. (c) Na depletion stimulates the forward trafficking of mature ENaC from ER to apical membrane. These findings are discussed in the following sections.

Two pathways for ENaC trafficking

The identification of both EndoH-sensitive and insensitive forms of ENaC at the cell surface in vivo agrees with a previous study on the processing of subunits expressed in Madin-Darby canine kidney cells (Hughey et al., 2004b). The simplest explanation is that ENaC can reach the cell surface by two routes. One is the classical pathway through the Golgi apparatus and entails posttranslational processing including mature glycosylation and cleavage of subunits by furin or other Golgi-resident proteases. A second pathway could bypass the Golgi altogether. This has been proposed previously for other membrane proteins including CFTR (Yoo et al., 2002), type I metalloprotease (Deryugina et al., 2004), and CD45 (Baldwin and Ostergaard, 2002). An alternative mechanism evokes transport through the Golgi in a form that is protected from both glycosylating and proteolytic enzymes. The significance of this unprocessed channel protein in the apical membrane is obscure.

The γENaC subunit is thought to be cleaved once by furin during transit through the Golgi and again after reaching the surface by extracellular proteases (Kleyman et al., 2009). Similar to previous studies (Frindt et al., 2008; Frindt and Palmer, 2009), we did not detect partially cleaved γENaC at the cell surface, although these forms could be seen in subcellular fractionations (Fig. S3), suggesting that the second cleavage step at the surface is rapid. Consistent with this, we found minimal effects of exogenous proteases on ENaC activity in split-open CCDs (Frindt et al., 2008). In contrast,

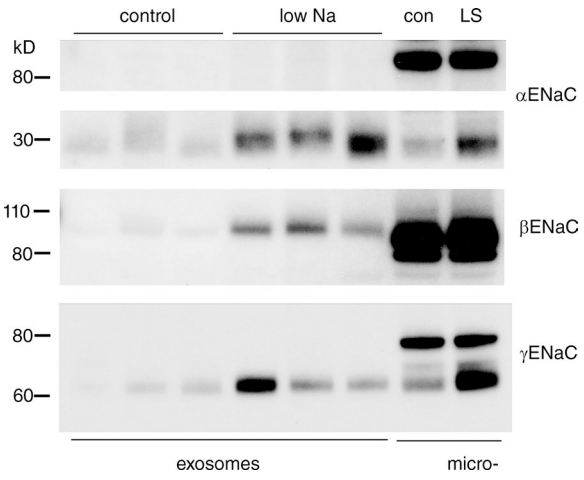

Figure 6. ENaC protein in urinary exosomes. Exosomes were sedimented from the urine of rats on control and low-Na diets. Each lane was loaded with exosomes from a volume of urine containing 70 µg creatinine. All the α- and γENaC protein that could be detected was in the fully cleaved form. The blots show results from four of eight pairs of animals. Na depletion increased the amount of all three ENaC subunits in exosomes, with mean values of low Na/control of 3.9 ± 0.7 for αENaC, 10.3 ± 3.3 for βENaC, and 4.5 ± 1.1 for γENaC.

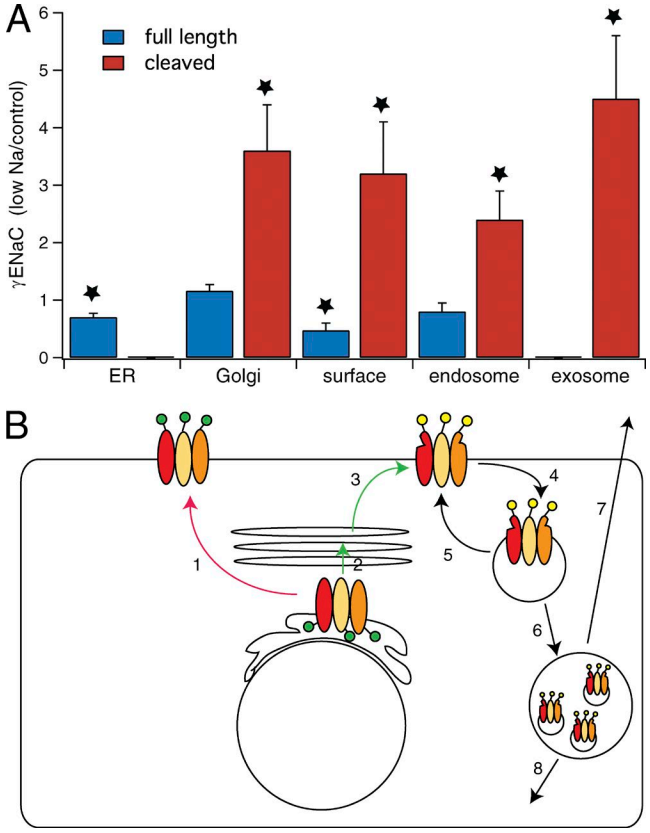

Figure 7. Fractional changes in full-length and cleaved γENaC in various membrane compartments in kidneys from Na-depleted versus control rats. (A) Compartments were identified by calnexin pull-down (ER, $n = 4$), GM130 pull-down (Golgi, $n = 3$), surface biotinylation (plasma membrane, $n = 4$), Rab11 pull-down (endosomes, $n = 4$), and exosomes ($n = 8$). Data are represented as mean ± SEM. *, $P < 0.05$ by t test. (B) Cartoon showing possible trafficking steps stimulated (green) or inhibited (red) by aldosterone/Na depletion. Step 1 is a putative alternative route from ER to the apical membrane that bypasses the final glycosylation and furin-dependent proteolysis of the Golgi apparatus. It appears to be slowed with Na depletion. Step 2 is transfer from ER to Golgi and may be stimulated by Na depletion. Step 3 is trafficking of cleaved and glycosylated protein from Golgi to apical membrane; it is accelerated by low Na. Steps 4 and 5 represent retrieval of protein into endosomes and recycling back to the surface. We cannot evaluate the effects of low Na on these steps. Endosomal retrieval is expected to increase caused by increased density of channels in the apical membrane. Steps 6 and 7 represent transfer to multivesicular bodies and release into the urine as exosomes. These rates also may be increased by the amount of protein in the endosomes. Step 8 represents eventual degradation.

another study (Nesterov et al., 2008) reported mild activation of ENaC currents by trypsin in microdissected mouse CCDs. Furthermore, chymotrypsin stimulated ENaC-dependent Na reabsorption in microperfused late distal convoluted tubules in rat kidney (Jacquillet et al., 2013). In both cases, the effects of proteases were variable and the mean activation was only 10–30%. It is possible that such activation, when present, reflects cleavage of intact γ subunits that were not cleaved by furin (Hughey et al., 2004a).

Na depletion selectively stimulates trafficking of mature subunits

Na depletion stimulates the transport of ENaC through the classical pathway involving export from the ER, processing in the Golgi, insertion into the plasma membrane, and retrieval by endosomes. This presumably reflects the actions of the mineralocorticoid aldosterone, which has similar effects on ENaC cleavage (Masilamani et al., 1999; Ergonul et al., 2006) and surface expression (Frindt et al., 2008). The abundance of the fully processed forms of α, β, and γ subunits increases, whereas that of the incompletely processed forms is variable, with no clear correlation with dietary Na intake. Thus, the fully processed species, both in the total cell extract and at the surface, correlates with the physiological status of the channels.

Stoichiometry of subunit trafficking

Previous studies presented evidence for noncoordinated trafficking of ENaC subunits (Weisz and Johnson, 2003). In particular, different subunits had different lifetimes at the cell surface in some (Weisz et al., 2000), but not in other (Alvarez de la Rosa et al., 2002), studies. In our previous measurements of cell-surface expression of ENaC in rat kidney, we found smaller fractional changes in βENaC compared with γENaC (Frindt et al., 2008; Frindt and Palmer, 2009), consistent with the idea that either insertion or retrieval of subunits could be independent of each other. In this paper, we report similar changes at the surface for the mature, presumably active forms of all the three subunits. On the other hand, immature subunits show different surface expression patterns in response to Na depletion. We think that the simplest explanation for these observations is that ENaC can assemble, presumably in the ER, with different subunit stoichiometries. Those with the "correct" stoichiometry move preferentially through the canonical Golgi pathway. Those with alternative stoichiometries may use the alternative route. It is also possible that channels with different subunit compositions have different rates of retrieval from the membrane. This scheme could account for variable changes in subunit expression and lifetimes under some conditions.

Redistribution of ENaC

Immunocytochemistry (Masilamani et al., 1999; Loffing et al., 2000, 2001) indicated that under control conditions, much of the ENaC protein is in intracellular membranes, moving to the surface with mineralocorticoid stimulation. The finding that β and γENaC increased at the surface in the absence of large changes in overall content of the subunits is consistent with this idea (Frindt et al., 2008; Frindt and Palmer, 2009). The precise intracellular locations of ENaC in the unstimulated state are unresolved. In the case of the γENaC subunit, the majority of the protein remains unprocessed under these conditions; at least part of this population resides in the ER (Fig. 4). However we could account for only ∼10% of the full-length ENaC in the ER fraction (Fig. S4). Much of the γENaC in the Golgi was also in the unprocessed state, but the total amount in this fraction was also small and, if anything, increased (low Na/control = 1.16 ± 0.11, $n = 3$) with Na depletion (Fig. 5). It is possible that some of the unprocessed ENaC protein resides in a subcompartment of ER that does not express calnexin. Alternatively, it may be in a compartment that we have not yet identified.

Mechanism of control of ENaC surface expression

Previous work has suggested a mechanism of regulation of ENaC activity and surface expression by aldosterone that involves inhibition of channel retrieval from the apical membrane (Staub et al., 2000; Snyder et al., 2002; Snyder, 2005). In this scheme, aldosterone induces the expression of SGK1, which phosphorylates the ubiquitin ligase Nedd4-2. In this phosphorylated form, Nedd4-2 binding to cytoplasmic C termini of ENaC is abrogated, and the reduced ubiquitination results in longer lifetimes of the subunits at the surface. Our findings do not rule out such mechanism, although they do indicate that increased ENaC abundance at the surface does not come at the expense of that in Rab11-containing endosomes. Previous studies showed that this compartment contains ENaC and likely served as a source for both basal and cAMP-dependent channel insertion into the membrane (Butterworth et al., 2012). Na depletion led to parallel changes in the content of ENaC in the Rab11 vesicles and the plasma membrane. This could be explained if increased surface expression pushes more ENaC into the recycling endosomes. However, the data are equally consistent with a scheme in which increased content of the Rab11 compartment drives the rise in apical membrane expression.

Our results argue that stimulation of trafficking to the apical membrane is an important component of the regulatory process. This conclusion is based on three lines of evidence. First, the amount of full-length γENaC protein in the ER fraction decreased with stimulation. This is consistent with acceleration of movement from ER to Golgi. Second, the amount of cleaved γENaC in

the Golgi increased in parallel with the increase in fully cleaved subunit at the surface. Finally, in the steady state, the amount of processed ENaC excreted in exosomes increased, suggesting a concomitant increase in the production of the processed forms.

Increased forward trafficking of ENaC could arise from several mechanisms. In principle, the rate of protein synthesis could be increased, as proposed for A6 cells (May et al., 1997). This seems unlikely in the case of the rat kidney, as the abundance of γENaC in the ER fraction decreased rather than increased. Transit of the protein from ER to Golgi could also be accelerated, which is consistent with the observed decrease in ENaC in the ER. However, the analysis of Golgi membranes indicates that this is not the only effect. The total content of γENaC was only slightly increased, whereas the amount of processed (cleaved) subunit was much higher. This could reflect induction or activation of enzymes responsible for proteolytic cleavage of the channels, and the cleaved subunits might be preferentially delivered to the apical membrane. However, the main intracellular protease cleaving ENaC is thought to be furin (Hughey et al., 2004a), and we are unaware of any evidence that aldosterone increases the expression of this intracellular protease. Alternatively, increased processing could reflect movement of the channels from cis- to trans-Golgi, where furin is predominately expressed (Molloy et al., 1999). Here, the greater abundance of fully processed subunits is a consequence rather than the cause of enhanced trafficking. These scenarios are compatible with the proposal (Liang et al., 2010) that aldosterone promotes forward trafficking to the membrane from an unspecified intracellular compartment under the influence of the induced proteins SGK1, a serine/threonine kinase, and the Rab-GTPase activator protein AS160. In any case, acceleration of movement of ENaC through the Golgi would lead to enhanced accumulation of fully processed subunits as well as increased surface density of active channels.

We dedicate this work to the memory of Haim Garty (1948–2014), a cherished colleague whose work in this field was cut short.

This work was supported by National Institutes of Health grants DK27847 and DK 099284 (to L.G. Palmer) and GM 314107 (to E. Rodriguez-Boulan, providing salary support for D. Gravotta).

The authors declare no competing financial interests.

Laurent Schild served as guest editor.

Submitted: 19 October 2015
Accepted: 11 January 2016

REFERENCES

Alvarez de la Rosa, D., H. Li, and C.M. Canessa. 2002. Effects of aldosterone on biosynthesis, traffic, and functional expression of epithelial sodium channels in A6 cells. *J. Gen. Physiol.* 119:427–442. http://dx.doi.org/10.1085/jgp.20028559

Asher, C., H. Wald, B.C. Rossier, and H. Garty. 1996. Aldosterone-induced increase in the abundance of Na^+ channel subunits. *Am. J. Physiol.* 271:C605–C611.

Baldwin, T.A., and H.L. Ostergaard. 2002. The protein-tyrosine phosphatase CD45 reaches the cell surface via golgi-dependent and -independent pathways. *J. Biol. Chem.* 277:50333–50340. http://dx.doi.org/10.1074/jbc.M209075200

Butterworth, M.B., R.S. Edinger, M.R. Silvis, L.I. Gallo, X. Liang, G. Apodaca, R.A. Frizzell, and J.P. Johnson. 2012. Rab11b regulates the trafficking and recycling of the epithelial sodium channel (ENaC). *Am. J. Physiol. Renal Physiol.* 302:F581–F590. http://dx.doi.org/10.1152/ajprenal.00304.2011

Casanova, J.E., X. Wang, R. Kumar, S.G. Bhartur, J. Navarre, J.E. Woodrum, Y. Altschuler, G.S. Ray, and J.R. Goldenring. 1999. Association of Rab25 and Rab11a with the apical recycling system of polarized Madin-Darby canine kidney cells. *Mol. Biol. Cell.* 10:47–61. http://dx.doi.org/10.1091/mbc.10.1.47

Deryugina, E.I., B.I. Ratnikov, Q. Yu, P.C. Baciu, D.V. Rozanov, and A.Y. Strongin. 2004. Prointegrin maturation follows rapid trafficking and processing of MT1-MMP in Furin-Negative Colon Carcinoma LoVo Cells. *Traffic.* 5:627–641. http://dx.doi.org/10.1111/j.1600-0854.2004.00206.x

Ergonul, Z., G. Frindt, and L.G. Palmer. 2006. Regulation of maturation and processing of ENaC subunits in the rat kidney. *Am. J. Physiol. Renal Physiol.* 291:F683–F693. http://dx.doi.org/10.1152/ajprenal.00422.2005

Escoubet, B., C. Coureau, J.P. Bonvalet, and N. Farman. 1997. Noncoordinate regulation of epithelial Na channel and Na pump subunit mRNAs in kidney and colon by aldosterone. *Am. J. Physiol.* 272:C1482–C1491.

Frindt, G., and L.G. Palmer. 2009. Surface expression of sodium channels and transporters in rat kidney: effects of dietary sodium. *Am. J. Physiol. Renal Physiol.* 297:F1249–F1255. http://dx.doi.org/10.1152/ajprenal.00401.2009

Frindt, G., and L.G. Palmer. 2012. Regulation of epithelial Na+ channels by adrenal steroids: mineralocorticoid and glucocorticoid effects. *Am. J. Physiol. Renal Physiol.* 302:F20–F26. http://dx.doi.org/10.1152/ajprenal.00480.2011

Frindt, G., Z. Ergonul, and L.G. Palmer. 2008. Surface expression of epithelial Na channel protein in rat kidney. *J. Gen. Physiol.* 131:617–627. http://dx.doi.org/10.1085/jgp.200809989

Garty, H., and L.G. Palmer. 1997. Epithelial sodium channels: function, structure, and regulation. *Physiol. Rev.* 77:359–396.

Hughey, R.P., G.M. Mueller, J.B. Bruns, C.L. Kinlough, P.A. Poland, K.L. Harkleroad, M.D. Carattino, and T.R. Kleyman. 2003. Maturation of the epithelial Na^+ channel involves proteolytic processing of the alpha- and gamma-subunits. *J. Biol. Chem.* 278:37073–37082. http://dx.doi.org/10.1074/jbc.M307003200

Hughey, R.P., J.B. Bruns, C.L. Kinlough, K.L. Harkleroad, Q. Tong, M.D. Carattino, J.P. Johnson, J.D. Stockand, and T.R. Kleyman. 2004a. Epithelial sodium channels are activated by furin-dependent proteolysis. *J. Biol. Chem.* 279:18111–18114. http://dx.doi.org/10.1074/jbc.C400080200

Hughey, R.P., J.B. Bruns, C.L. Kinlough, and T.R. Kleyman. 2004b. Distinct pools of epithelial sodium channels are expressed at the plasma membrane. *J. Biol. Chem.* 279:48491–48494. http://dx.doi.org/10.1074/jbc.C400460200

Jacquillet, G., H. Chichger, R.J. Unwin, and D.G. Shirley. 2013. Protease stimulation of renal sodium reabsorption in vivo by activation of the collecting duct epithelial sodium channel (ENaC). *Nephrol. Dial. Transplant.* 28:839–845. http://dx.doi.org/10.1093/ndt/gfs486

Kellenberger, S., and L. Schild. 2002. Epithelial sodium channel/degenerin family of ion channels: a variety of functions for a shared structure. *Physiol. Rev.* 82:735–767. http://dx.doi.org/10.1152/physrev.00007.2002

Kleyman, T.R., M.D. Carattino, and R.P. Hughey. 2009. ENaC at the cutting edge: regulation of epithelial sodium channels

by proteases. *J. Biol. Chem.* 284:20447–20451. http://dx.doi.org/10.1074/jbc.R800083200

Liang, X., M.B. Butterworth, K.W. Peters, and R.A. Frizzell. 2010. AS160 modulates aldosterone-stimulated epithelial sodium channel forward trafficking. *Mol. Biol. Cell.* 21:2024–2033. http://dx.doi.org/10.1091/mbc.E10-01-0042

Loffing, J., L. Pietri, F. Aregger, M. Bloch-Faure, U. Ziegler, P. Meneton, B.C. Rossier, and B. Kaissling. 2000. Differential subcellular localization of ENaC subunits in mouse kidney in response to high- and low-Na diets. *Am. J. Physiol. Renal Physiol.* 279:F252–F258.

Loffing, J., M. Zecevic, E. Féraille, B. Kaissling, C. Asher, B.C. Rossier, G.L. Firestone, D. Pearce, and F. Verrey. 2001. Aldosterone induces rapid apical translocation of ENaC in early portion of renal collecting system: possible role of SGK. *Am. J. Physiol. Renal Physiol.* 280:F675–F682.

Maley, F., R.B. Trimble, A.L. Tarentino, and T.H. Plummer Jr. 1989. Characterization of glycoproteins and their associated oligosaccharides through the use of endoglycosidases. *Anal. Biochem.* 180:195–204. http://dx.doi.org/10.1016/0003-2697(89)90115-2

Masilamani, S., G.H. Kim, C. Mitchell, J.B. Wade, and M.A. Knepper. 1999. Aldosterone-mediated regulation of ENaC alpha, beta, and gamma subunit proteins in rat kidney. *J. Clin. Invest.* 104:R19–R23. http://dx.doi.org/10.1172/JCI7840

Matsuda, Y., A. Tsuji, T. Kuno, and N. Katunuma. 1983. Biosynthesis and degradation of gamma-glutamyltranspeptidase of rat kidney. *J. Biochem.* 94:755–765.

May, A., A. Puoti, H.P. Gaeggeler, J.D. Horisberger, and B.C. Rossier. 1997. Early effect of aldosterone on the rate of synthesis of the epithelial sodium channel alpha subunit in A6 renal cells. *J. Am. Soc. Nephrol.* 8:1813–1822.

McKee, J.A., S. Kumar, C.A. Ecelbarger, P. Fernández-Llama, J. Terris, and M.A. Knepper. 2000. Detection of Na(+) transporter proteins in urine. *J. Am. Soc. Nephrol.* 11:2128–2132.

Molloy, S.S., E.D. Anderson, F. Jean, and G. Thomas. 1999. Bi-cycling the furin pathway: from TGN localization to pathogen activation and embryogenesis. *Trends Cell Biol.* 9:28–35. http://dx.doi.org/10.1016/S0962-8924(98)01382-8

Nesterov, V., A. Dahlmann, M. Bertog, and C. Korbmacher. 2008. Trypsin can activate the epithelial sodium channel (ENaC) in microdissected mouse distal nephron. *Am. J. Physiol. Renal Physiol.* 295:F1052–F1062. http://dx.doi.org/10.1152/ajprenal.00031.2008

Pácha, J., G. Frindt, L. Antonian, R.B. Silver, and L.G. Palmer. 1993. Regulation of Na channels of the rat cortical collecting tubule by aldosterone. *J. Gen. Physiol.* 102:25–42. http://dx.doi.org/10.1085/jgp.102.1.25

Pisitkun, T., R.F. Shen, and M.A. Knepper. 2004. Identification and proteomic profiling of exosomes in human urine. *Proc. Natl. Acad. Sci. USA.* 101:13368–13373. http://dx.doi.org/10.1073/pnas.0403453101

Snyder, P.M. 2005. Minireview: regulation of epithelial Na^+ channel trafficking. *Endocrinology.* 146:5079–5085. http://dx.doi.org/10.1210/en.2005-0894

Snyder, P.M., D.R. Olson, and B.C. Thomas. 2002. Serum and glucocorticoid-regulated kinase modulates Nedd4-2-mediated inhibition of the epithelial Na+ channel. *J. Biol. Chem.* 277:5–8. http://dx.doi.org/10.1074/jbc.C100623200

Staub, O., I. Gautschi, T. Ishikawa, K. Breitschopf, A. Ciechanover, L. Schild, and D. Rotin. 1997. Regulation of stability and function of the epithelial Na+ channel (ENaC) by ubiquitination. *EMBO J.* 16:6325–6336. http://dx.doi.org/10.1093/emboj/16.21.6325

Staub, O., H. Abriel, P. Plant, T. Ishikawa, V. Kanelis, R. Saleki, J.D. Horisberger, L. Schild, and D. Rotin. 2000. Regulation of the epithelial Na+ channel by Nedd4 and ubiquitination. *Kidney Int.* 57:809–815. http://dx.doi.org/10.1046/j.1523-1755.2000.00919.x

Stokes, J.B., and R.D. Sigmund. 1998. Regulation of rENaC mRNA by dietary NaCl and steroids: organ, tissue, and steroid heterogeneity. *Am. J. Physiol.* 274:C1699–C1707.

Trischler, M., W. Stoorvogel, and O. Ullrich. 1999. Biochemical analysis of distinct Rab5- and Rab11-positive endosomes along the transferrin pathway. *J. Cell Sci.* 112:4773–4783.

Verrey, F., E. Hummler, L. Schild, and B.C. Rossier. 2008. Mineralocorticoid action in the aldosterone-sensitive distal nephron. *In* The Kidney: Physiology and Pathophysiology. Fourth edition. R.J. Alpern, and S.C. Hebert, editors. Academic Press, Burlington, MA. 889–924.

Wang, X., R. Kumar, J. Navarre, J.E. Casanova, and J.R. Goldenring. 2000. Regulation of vesicle trafficking in madin-darby canine kidney cells by Rab11a and Rab25. *J. Biol. Chem.* 275:29138–29146. http://dx.doi.org/10.1074/jbc.M004410200

Weisz, O.A., and J.P. Johnson. 2003. Noncoordinate regulation of ENaC: paradigm lost? *Am. J. Physiol. Renal Physiol.* 285:F833–F842. http://dx.doi.org/10.1152/ajprenal.00088.2003

Weisz, O.A., J.M. Wang, R.S. Edinger, and J.P. Johnson. 2000. Non-coordinate regulation of endogenous epithelial sodium channel (ENaC) subunit expression at the apical membrane of A6 cells in response to various transporting conditions. *J. Biol. Chem.* 275:39886–39893. http://dx.doi.org/10.1074/jbc.M003822200

Yoo, J.S., B.D. Moyer, S. Bannykh, H.M. Yoo, J.R. Riordan, and W.E. Balch. 2002. Non-conventional trafficking of the cystic fibrosis transmembrane conductance regulator through the early secretory pathway. *J. Biol. Chem.* 277:11401–11409. http://dx.doi.org/10.1074/jbc.M110263200